ELSEVIER

Biochimica et Biophysica Acta 1498 (2000) 181–191

BIOCHIMICA ET BIOPHYSICA ACTA

BBA

www.elsevier.com/locate/bba

S100 protein–annexin interactions: a model of the (Anx2-p11)$_2$ heterotetramer complex

Jana Sopkova-de Oliveira Santos [a,*], Frank K. Oling [b], Stéphane Réty [1,a], Alain Brisson [b], Jeremy C. Smith [c], Anita Lewit-Bentley [a]

[a] *L.U.R.E., CNRS, CEA, MENRT, Centre Universitaire Paris-Sud, Bâtiment 209D, B.P. 34, 91898 Orsay Cedex, France*

[b] *Departement of Chemistry/Biophysical Chemistry, BIOSON Institute GBB, University of Groningen, Nijenborgh 4, NL-9747 AG Groningen, The Netherlands*

[c] *Lehrstuhl für Biocomputing, IWR der Universität Heidelberg, D-69120 Heidelberg, Germany*

Received 11 September 2000; accepted 12 September 2000

Abstract

The (Anx2)$_2$(p11)$_2$ heterotetramer has been implicated in endo- and exocytosis in vivo and in liposome aggregation in vitro. Here we report on the modelling of the heterotetramer complex using docking algorithms. Two types of models are generated–heterotetramer and heterooctamer. On the basis of the agreement between the calculated (X-ray) electron density and the observed projected density from cryo-electron micrographs on the one hand, and calculated energy criteria on the other hand, the heterotetramer models are proposed as the most probable, and one of them is selected as the best model. Analysis of this model at an atomic level suggests that the interaction between the Anx2 core and p11 has an electrostatic character, being stabilised primarily through charged residues.

Keywords: p11 dimer; Annexin Anx2; Heterotetramer; Protein docking

1. Introduction

Membrane fusion is one of the key events in endo- and exocytosis in cells. In vivo, membrane fusion is controlled by several factors involving mainly calcium ions, proteins or protein modifications [1]. Several members of the annexin family of proteins, whose precise physiological functions remain unclear, have been implicated in this membrane traffic by the results of in vitro and in vivo experiments [2,3]. In particular, the (Anx2)$_2$(p11)$_2$ tetramer has been shown to aggregate chromaffin granules and has been localised to endosome membranes [4]. The (Anx2)$_2$(p11)$_2$ complex has also been shown to mediate in vitro Ca^{2+}-dependent aggregation of liposomes [3]. The formation of junctions between liposomes in the presence of (Anx2)$_2$(p11)$_2$ has been studied recently by electron microscopy [5]. The images show the two lipid membranes bridged by the (Anx2)$_2$(p11)$_2$ complex which forms well-ordered two-dimensional arrays.

All annexin family members bind to negatively charged phospholipid membranes in a Ca^{2+}-dependent manner [6]. Annexins possess a conserved core domain, consisting of four or eight homologous seg-

* Corresponding author. C.E.R.M.N., UFR des Sciences Pharmaceutiques, 5 rue Vaubénard, 14032 Caen, France. Fax: +33-2-3193-1188;
E-mail: sopkova@pharmacie.unicaen.fr

[1] Present address: Laboratoire de Biologie Moleculaire et Cellulaire, ENS Lyon, 46 allée d'Italie, 69364 Lyon, France.

0167-4889/00/$ – see front matter
PII: S0167-4889(00)00095-1

ments of 70 amino acid residues, and an N-terminal domain which varies both in its length and composition. While the conserved core is responsible for the interaction of annexins with the calcium and membranes, their specific functions are controlled by the variable N-terminal domains [7]. In particular, the latter carry the sites of post-translational modifications, such as myristoylation and phosphorylation, as well as the site of interaction with other proteins. It has been shown that several annexins form complexes with proteins from the S100 EF-hand Ca^{2+}-binding protein family, e.g., Anx1 with S100C (S100A11) [8], Anx2 with p11 (S100A10) [9] and Anx11 with calcyclin (S100A6) [10].

Mutagenesis studies have shown that the p11 binding site of Anx2 lies in the first 14 amino acids of the N-terminal domain, which forms an amphipathic α-helix [11]. The structure of the p11 dimer, as well as the structure of the complex of p11 with a synthetic peptide corresponding to the first 13 amino acids of the Anx2 N-terminus, have been determined in our laboratory [12]. The amphipathic helix lies in a hydrophobic cleft formed by loop L_2 and C-terminal helix H_{IV} of one p11 molecule and N-terminal helix H_I of the other p11 monomer. The structure confirms and explains results obtained earlier on the regions important for complex stability on Anx2, in particular the N-acetyl group of Ser 1 and the hydrophobic side chains, Val 3, Ile 6, Leu 7 and Leu 10 on one side of the N-terminal α-helix [11,13]. In the structure these residues are in contact with the p11 surface. The corresponding annexin binding site on p11, that had been determined by progressively truncating p11 molecules [14], concerns a highly hydrophobic region located in the C-terminal extension between residues 85 and 91 (helix H_{IV}). Furthermore, Cys 82, whose modification abolishes Anx2 binding, also lies in the binding site [15]. The structure also confirms the importance of hydrophobic residues in the N-terminal helix of p11, as well as in the loop connecting the two EF-hands, in the stability of the complex.

The coordinates of the p11–peptide complex, together with those of the Anx2 structure (without the N-terminal domain [16]), have provided the basis for modelling the $(Anx2)_2(p11)_2$ tetramer at atomic detail. Two different $(Anx2)_2(p11)_2$ models have been proposed to date. The first one is based on a cryo-electron microscopy study of junctions between phospholipid vesicles coated with the Anx2:p11 complex in the presence of calcium [5]. The electron density profile of these junctions consists of seven bands which were interpreted as follows: the two external bands on both sides correspond to the headgroups of the two lipid layers, while the three bands in the centre of the junction correspond to the Anx2:p11 complex. This complex is proposed to have the dimer of p11 in the centre of the protein density, with one molecule of Anx2 on either side, i.e., (Anx2 band)–(p11 dimer band)–(Anx2 band). Furthermore, the electron microscopy study gave an estimate of the dimension of the complex attached to the membranes as 90 ± 3 Å and an estimate of the distance between the centres of gravity of each Anx2 band and that of the central $(p11)_2$ band as 30 ± 5 Å [5].

The second model, as proposed by Waisman [17], has two molecules of Anx2 lying on the same side of the p11 dimer. In order to link two membrane surfaces, the model assumes two such heterotetramers forming effectively an octameric structure, which is held together through the p11 dimer. In both the crystal structure of p11 alone, as well as in the complex of p11 with the N-terminus of Anx2, the dimers of p11 do indeed form a tetramer via a disulfide bridge between their Cys 61.

The information from X-ray crystallography, combined with the electron microscopy results described above, provides a collection of data on which modelling studies can be based in order to obtain atomic detail structural information on the functional $(Anx2)_2(p11)_2$ complex.

2. Materials and methods

All calculations were performed using version 23 of the programme CHARMM [18] and the programme DOCK [19,20], with the exception of some preliminary coordinate manipulations and Fourier transformation calculations for which programmes from the CCP4 package were used [21].

2.1. Model structures

The heterotetramer modelling was performed using the crystal structure of Anx2 determined earlier

(coordinates provided by A. Hofmann) [16], in which the entire N-terminus is absent (up to residue 33), and that of the complex of p11 dimer with the Anx2 N-terminus peptide (PDB entry 1BT6) [12]. Since mutagenesis results as well as the structure of the complex indicate that the N-terminus acetylation is necessary for interaction with the p11 dimer [11], the acetyl group was conserved.

2.2. Docking procedure

The algorithm used in the docking calculations is based on simplified protein models in which each amino acid residue is replaced by a sphere centred on the centre of gravity of its side chain [19,20]. Both molecules tested are considered as rigid bodies, and their relative positions are described by six degrees of freedom: five angles and their mutual distance. The quality of the modelled complexes is evaluated by an energy term of the following form:

$$E_B = E^* - \gamma B^* \quad (1)$$

where E^* is an approximate repulsive energy and γB^* represents the attractive energy due to buried surface area B^* of the components of the complex. The constant γ converts a surface area into an energy and has the dimension of surface tension ($\gamma = 50$ kcal/mol per Å^2 in this calculation) [19]. Two procedures are possible in the docking programme: uniform sampling or simulated annealing. The latter employs a Monte Carlo algorithm, and permits the sampling of many deep local minima [19].

The docking method was used to search for the optimal position of one monomer of Anx2 (without its N-terminal part [16]) with respect to the crystal structure of the p11 dimer in complex with the amphipathic N-terminal of Anx2 [12]. Thus in our models there are 22 amino acids of the Anx2 N-terminal domain missing. The calculations were performed using both docking approaches, grid search (GS) and simulated annealing (SA).

2.3. Calculation of two-dimensional projection electron density maps from generated models

For the Fourier transform calculations the models were oriented with the highest symmetry axis of the p11 dimer parallel to the z-axis, with their longer axis oriented parallel to the x-axis. Fourier transform of the models was calculated (program SFALL [21]) and sampled by the reciprocal lattice of a minimal box containing each model, giving a set of (h, k, l, amplitude, phase) structure factors. A two-dimensional projection map was calculated by limiting the resolution to 20 Å and the structure factor list to (h, k, $l = 0$) terms, using a suite of modified IMAGIC and MRC programmes.

2.4. Refinement of the models at atomic detail. Energy minimisation procedure

The rigid-body docking programme allows an initial estimation of the relative positions of the molecules. Refinement of the models was subsequently carried out at atomic resolution using energy minimisation with the programme CHARMM [18] and parameter set 22 [22]. The model system consisted of all heavy atoms of the proteins and all hydrogens. The potential energy function contains bonded terms representing bond length, valence angle and torsional (dihedral) angle variations and non-bonded (van der Waals and electrostatic) interactions. The van der Waals interactions were truncated using a switching function between 11 and 14 Å and the electrostatic interactions were smoothly brought to zero at 14 Å using a shifting function [18].

In the energy minimisation calculations all residues further than 15 Å from the Anx2–p11 interface were kept fixed and the models were minimised to an RMS energy gradient $< 10^{-2}$ kcal/(mol Å). Several properties of the resulting atomic models were examined. Among these were the interaction energies of Anx2 core with the p11 dimer, calculated as the sum of van der Waals and electrostatic energies of the CHARMM potential function between atoms of both components of the complex. We also determined contact residues between the helix and the dimer, by calculations of the contribution of individual amino acids to the total interaction energy and by calculations of the distances of contact atoms between Anx2 and p11.

3. Results

The approach taken in this work was to generate

model complexes using the docking procedure, to rank and refine them by energy minimisation, and finally to compare them with known experimental data.

3.1. Complex of the p11 dimer with Anx2

Using the criteria of buried surface area $B^* > 1500$ Å^2 and energy $E_B < -50$ kcal/mol, 363 models were selected for the grid search and 385 models were selected for the simulated annealing procedure (see Table 1). In both cases, the models were divided into 10 clusters with similar Anx2 positions with respect to the p11 dimer. One representative structure was generated for each cluster. For each selected model the whole tetramer was constructed by applying the internal twofold symmetry of the p11 dimer to the Anx2 molecules. From these tetramers we selected those with no overlap of Anx2 monomers (see 'overlap' remark in Table 1) and for which the calcium sites of Anx2 were not in contact with the p11 dimer (see Table 1: 'Ca sites' remark). Six models in total were retained from the grid search and four from simulated annealing.

Fig. 1. Ribbon representation of hetero-octamer models of $(Anx2)_2(p11)_2$. (A) Heterotetramer model 1 from grid search; (B) corresponding hetero-octamer model. (C) Heterotetramer model 8 from simulated annealing search; (D) corresponding hetero-octamer model. Anx2, light grey; p11 dimer, black and white; Anx2 N-terminal peptides, dark grey. Cys 61 of the p11 is in the ball-and-stick representation.

→

One of the experimental criteria for further selection of models for the $(Anx2)_2(p11)_2$ complex was the distance between the centres of gravity of the Anx2 and p11 dimer bands, which is 30 ± 5 Å as estimated from the cryo-electron microscopic junction study [5]. We therefore calculated the distances between the centres of gravity of the Anx2 molecules and p11 dimer for each model (see Table 1) and compared them with the experimental values. Only GS complexes 1 and 2 and SA complexes 1, 2, 7 and

Table 1
The energetic and positional characteristics of models of the $(Anx2)_2(p11)_2$ heterotetramer calculated by the docking programme

	Average buried surface area (Å^2)	Mean energy of cluster (kcal/mol)	D (Å)[a]	Remarks
(A) Grid search				
Cluster 1	1868	−85.3	33.3[b]	
Cluster 2	1654	−78.2	33.5	
Cluster 3	1801	−81.8	–	None (overlap)
Cluster 4	1699	−79.4	–	None (overlap)
Cluster 5	1916	−83.4	37.6	$D \gg 30$
Cluster 6	1839	−81.8	–	None (overlap)
Cluster 7	1809	−82.0	–	None (Ca sites)
Cluster 8	1723	−76.5	–	None (Ca sites)
Cluster 9	1691	−75.4	–	None (Ca sites)
Cluster 10	1645	−75.1	40.9	$D \gg 30$
(B) Simulated annealing				
Cluster 1	1785	−82.6	33.4[b]	
Cluster 2	1660	−78.6	33.7	
Cluster 3	1634	−76.6		None (overlap)
Cluster 4	1816	−81.4		None (overlap)
Cluster 5	1541	−72.7		None (overlap)
Cluster 6	1863	−81.2	37.6	$D \gg 30$
Cluster 7	1875	−81.4	31.9	
Cluster 8	1519	−72.6	34.7[b]	
Cluster 9	1727	−77.2		None (overlap)
Cluster 10	1665	−74.4		None (Ca sites)

[a] D is the distance between the centres of gravity of Anx2 and the p11 dimer.
[b] Distance D was calculated between the centres of gravity of two Anx2 molecules on the same side of the p11 tetramer and the p11 tetramer.

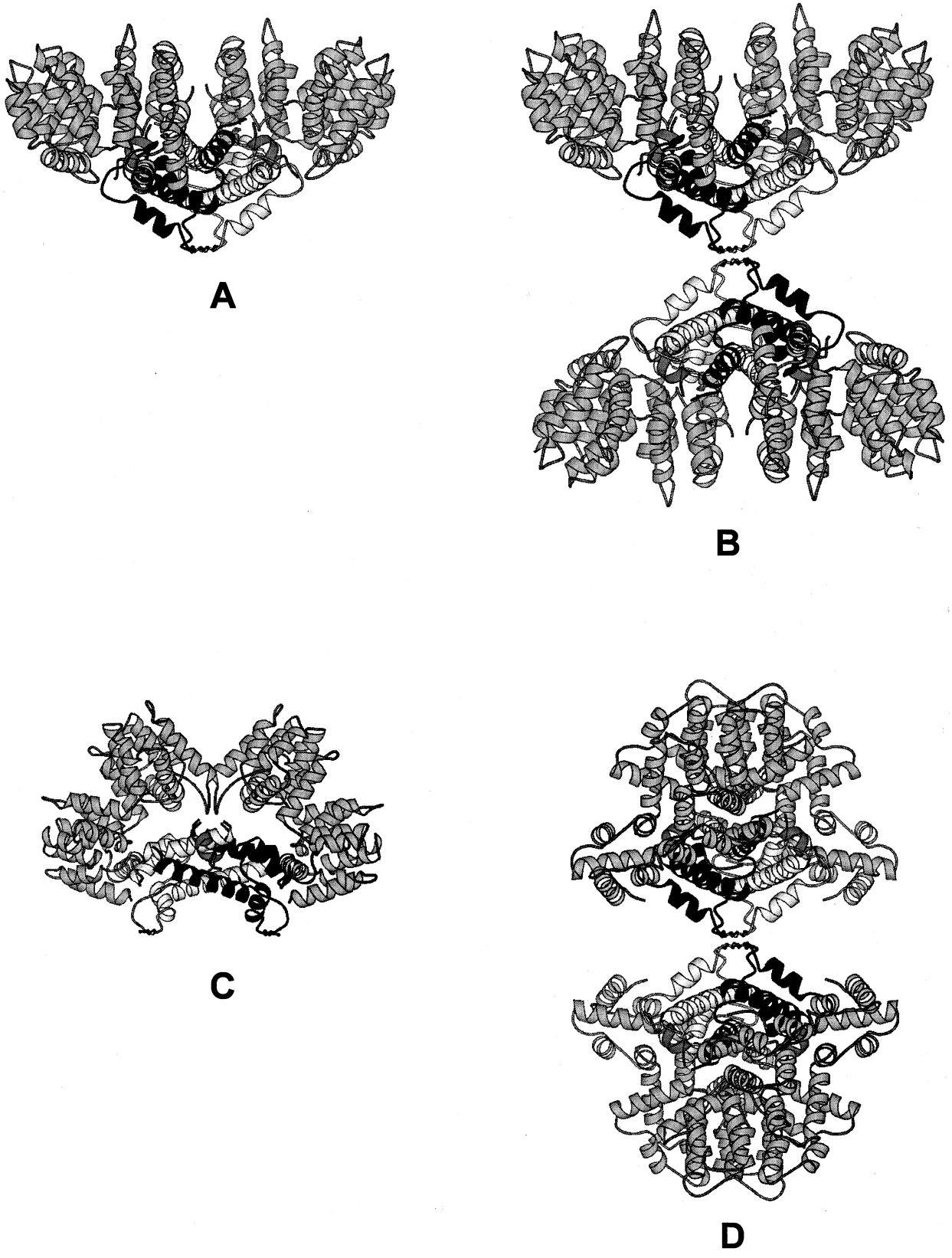
A
B
C
D

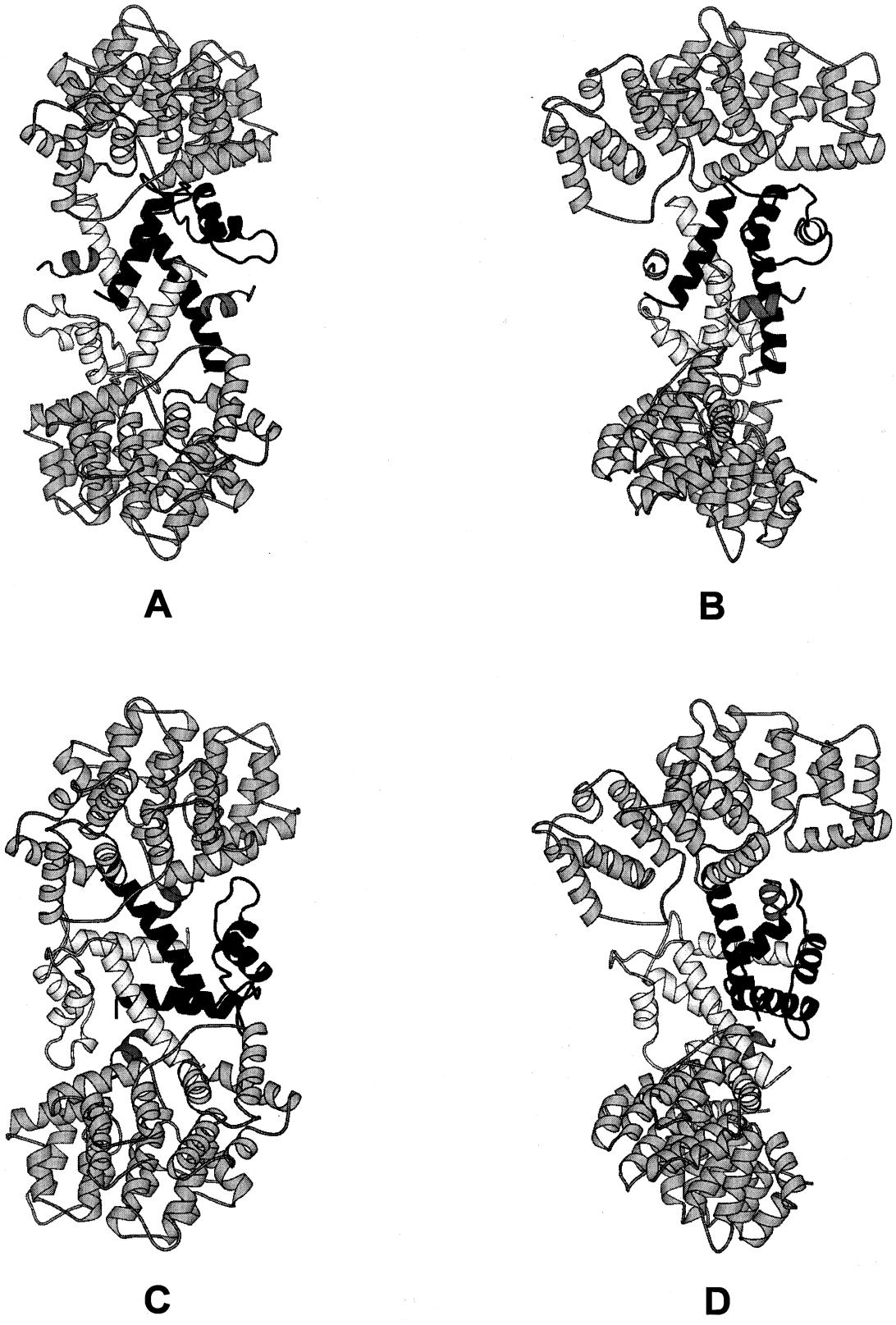
A
B
C
D

Fig. 2. Ribbon representation of heterotetramer models of $(Anx2)_2(p11)_2$. (A,B) Heterotetramer model 2 from simulated annealing in two different views. (C,D) Heterotetramer model 7 from simulated annealing in two different views. Anx2, light grey; p11 dimer, black and white; Anx2 N-terminal peptides, dark grey. (Figs. 1 and 2 were prepared with MOLSCRIPT [24]).
←

8 possess satisfactory values. Subsequent comparison of the grid search and simulated annealing models showed that GS model 1 is practically identical to SA model 1 (RMS of backbone atoms ~0.27 Å) and, similarly, GS model 2 corresponds to SA model 2 (backbone RMS ~0.27 Å). Below we shall therefore discuss only four models: GS 1 and SA 2, 7 and 8.

3.1.1. Hetero-octamer models

In the case of GS model 1 and SA model 8 the two molecules of Anx2 are situated in such a way that they can interact only with the same lipid layer (see Fig. 1A,C). For these models the only possibility of satisfying the observation of three bands in the junctions (Anx2–p11–Anx2) is through the mutual interaction of two heterotetramers. The observed junction profile of three bands might then correspond to (two Anx2 molecules)–(p11 homotetramer)–(two Anx2 molecules), which means that these models correspond to those suggested by Waisman [17]. The formation of junctions can be imagined through the interaction of two $(Anx2)_2(p11)_2$ heterotetramer intermediates. That this arrangement is plausible is supported by the observation of the formation of a p11 homotetramer via a disulfide bridge of Cys 61, both in the crystals of p11 alone and in the crystals of the complex of p11 with the Anx2 N-terminal peptide [12]. Furthermore, in both tetramer models GS 1 and SA 8 the Cys 61 side chains lie on the complex surface, in a position to interact with neighbouring heterotetramers by forming disulfide bridges between them (Fig. 1A). In the GS 1 and SA 8 models the Anx2 cores lie on the same side of p11 dimer, but their mutual orientation is somewhat different. The hetero-octamer can be constructed without any difficulty using the crystallographic p11 homotetramer (see Fig. 1B,D).

3.1.2. Heterotetramer models

Models SA 2 and SA 7 correspond to the complex configuration proposed by Lambert et al. [5], insofar as the relative orientation of the Anx2 and p11 dimer is such that the Anx2 molecules lie on opposite sides of the p11 dimer, with the convex, calcium binding sites at the top and bottom of the heterotetramer (see Fig. 2). Viewed as in Fig. 2B,D, the two Anx2 molecules are approximately perpendicular to each other. This constitutes novel information which could not be obtained in the cryo-electron microscopy analysis [5]. The principal difference between models SA 2 and SA 7 is in the position of Anx2 with respect to the p11 dimer (see Fig. 2A,C). In model SA 2 the Anx2 core lies in the proximity of loop L_1 and L_3 of the p11 dimer (see Fig. 2A), whereas in model SA 7 it lies in the proximity of the Anx2 N-terminal binding cavity (Fig. 2C).

3.2. Electron density profiles of the models

In order to compare the models with the available electron microscopy data, the projected electron density profile corresponding to each selected model was calculated and compared to the atomic potential map obtained by cryo-electron microscopy.

3.2.1. Hetero-octamer models

The calculated profile of densities, projected down and averaged about the fourfold axis of the p11 tetramer of the GS 1 model, shows essentially two bands separated by a region with no density (Fig. 3A). Each density band corresponds to one heterotetramer and it is impossible to distinguish Anx2 from p11 density.

The situation is similar for the calculated density profile of the second hetero-octamer model, SA 8. The model gives four bands in the electron density profile (Fig. 3B). Two bands characteristic of each heterotetramer and superimposable on each other are separated by a large region of low density corresponding to the centre of the p11 tetramer. The bands corresponding to molecules of Anx2 and the p11 dimer can be distinguished here.

We can conclude that these models do not give a three-band density junction profile corresponding to the experimental observations.

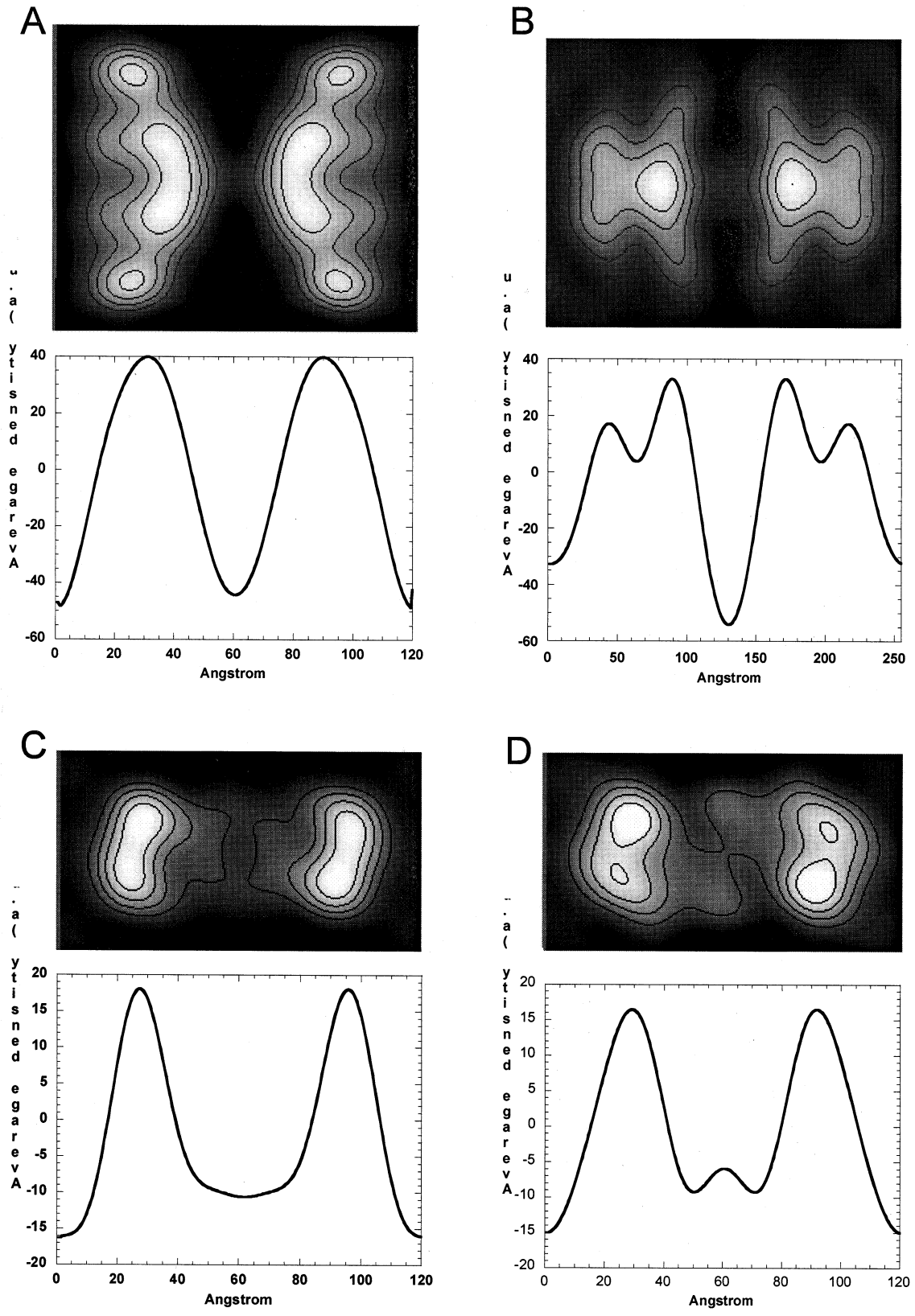
A
B
C
D
Angstrom
Angstrom
Angstrom
Angstrom

Fig. 3. The calculated two-dimensional electron density maps viewed down the internal twofold axis of the p11 dimer or the fourfold axis of the p11 tetramer (upper figures in A–D). The lower figures in A–D represent the histograms of the sums of densities projected down the vertical direction in these maps. (A) model GS 1, (B) model SA 8, (C) model SA 2, (D) model SA 7.
←

3.2.2. Heterotetramer models

The disposition of molecules in both heterotetramer models SA 2 and SA 7 could give rise to three independent density bands in the calculated electron density profile. However, the electron density corresponding to the p11 dimer is very low in the SA 2 model (Fig. 3C), thus forming in fact a two-band density profile. Only the SA 7 model gives rise to a true three-band density profile (Fig. 3D), and for this reason is selected as the most probable of the four. The observed distances between the density peaks in the histogram of the calculated density profile are very close to the experimentally observed values: the distance between the external and internal bands is about 31.4 Å (experimental value 30 ± 5 Å) and the distance between two external bands is about 62.8 Å (experimental value 60 ± 5 Å).

3.3. Stability of the model

We carried out a comparison of the models using energy criteria in order to evaluate their overall stability and the strength of interaction between their component molecules. The energy minimised models show that the interaction energy of Anx2 core with the p11 dimer is stronger in the heterotetramer than in the hetero-octamer models (Table 2). This makes the latter less probable from both the electron density profile and the energetic points of view. The difference in interaction energy of the two heterotetramer models is practically insignificant, with $\Delta E_{INT}(SA2-SA7)$ about 12 kcal/mol. It is therefore impossible to differentiate between the heterotetramer models using this criterion.

Table 2
Energy characteristics of heterotetramer $(Anx2)_2(p11)_2$ models after refinement by energy minimisation

	Interaction energy Anx2 core–p11 dimer (kcal/mol)
Model GS1	−156
Model SA2	−12
Model SA7	0
Model SA8	−170

In the SA 7 model the annexin core interacts with both molecules of the p11 dimer through two regions. Residues 138–149 in helix C of Anx2 domain II interact with the extremity of the L_2 loop (residues 44–46) and with residue 53 in helix H_{III} of one p11 molecule. The region between Anx2 residues 181–188, the linker between domains II and III, interacts with residues of loop L_3 (the second EF hand loop) of the second molecule of the p11 dimer. Furthermore, a very strong local interaction, which itself contributes about 30% of the total interaction energy, is seen for Lys 302 in the C-helix of domain IV of Anx2, which interacts with the C-terminal part of the first p11 molecule. Our model shows that residues Lys 46, Lys 53, Gln 69, Ser 70, His 89, Lys 91 of p11 and residues Gln 69, Gln 138, Glu 139, Glu 142, Glu 149, Asp 182, Ser 184, Lys 302 of Anx2 are crucial for the interaction. All these residues are charged, which means that in SA 7 the interaction of p11 with the Anx2 core is primarily of an electrostatic character.

4. Discussion

We propose a model of the $(annexin)_2(p11)_2$ heterotetramer complex generated from the three-dimensional structures of the (p11–Anx2 N-terminal) complex and of Anx2 (without the N-terminal part) determined by X-ray crystallography as a starting point. By comparison with electron microscopy results we have selected one model from all the candidates, model SA 7. This model gives rise to three bands in the calculated electron density profile, and for this model the distances between the bands are also in agreement with experimental values. In this model the Anx2 molecules lie on opposite sides of the p11 dimer, close to the region of the Anx2 N-terminal helix binding, and obey its twofold symmetry. The interaction between Anx2 and the p11 dimer has several interesting features. Within the Anx2 N-

terminal part (residues 1–11) the interaction is mainly hydrophobic, as suggested by earlier experiments and confirmed by the crystal structure of the complex [12]. Our model indicates, however, that beyond the very N-terminal α-helix, downstream from residue 33, the interactions stabilising the complex are mainly electrostatic, maintained by hydrogen bonds between charged residues.

Interestingly, the model selected on criteria of best fit with experimental data, does not have a significantly stronger interaction energy between the Anx2 core and p11 compared with the other models. This phenomenon could be a consequence of the 22 amino acids our models do not account for. The last five C-terminal amino acids of p11 are also missing in the p11–peptide structure and may play and important role in complex stabilisation. From the mutual position of molecules in model SA 7 it is probable that these residues participate in the interaction. The observation of a strong interaction between the Anx2 core and C-termini of the p11 molecules in model SA 7 could indicate why the presence of the C-terminal part (residues 85–91) of p11 is required for its interaction with Anx2 [14].

The crystal structure of the complex of S100C with annexin I N-terminal peptide has been solved recently [23]. Its structure is remarkably similar to that of the p11–Anx2 peptide complex, yet the binding between the annexin N-terminal domains and S100 proteins has been shown to be specific. At the level of the annexin termini, the only difference in the two complexes found was the interaction surface, which is significantly smaller in the S100C–annexin I peptide complex. Our present results indicate that there could be more specific interactions between annexins and their S100 partners concerning regions of the annexin molecules not described by crystal structures available to date. There are two differences on the annexin side: residues Gln 138 and Ser 184 correspond to Lys 147 and Gly 193 on Anx1. The differences in the contacting residues on the S100 molecules concern the C-terminal segment: Ser 70, His 89 and Lys 91 in p11 correspond to Glu, Ser and Gln in the S100C sequence. This could again point to the importance of the p11 C-terminus in target recognition, as well as suggesting that the specificity of interaction between annexins and their S100 protein partners may lie beyond the annexin N-termini.

Acknowledgements

We thank Dr Jacqueline Cherfils (Gif sur Yvette, France) for providing us with the docking programme, Dr Andreas Hofmann (MPI Martinsried) for Anx2 coordinates, and Dr Wilko Keegstra (University of Groningen) for expert technical assistance. J.S.-de O. was supported by EC programme BIOTECH no. BIO4CT960083.

References

[1] J.E. Rothman, Mechanism of intracellular protein transport, Nature 372 (1994) 55–63.
[2] C.E. Creutz, The annexins and endocytosis, Science 258 (1992) 924–931.
[3] V. Gerke, in: B.A. Seaton (Ed.), Annexins: Molecular Structure to Cellular Function, R.G. Landes, Austin, TX, 1992, pp. 67–75.
[4] V. Gerke, S. Moss, Annexins and membrane dynamics, Biochim. Biophys. Acta 1357 (1997) 129–154.
[5] O. Lambert, V. Gerke, M.-F. Bader, F. Porter, A. Brisson, Structural analysis of junctions formed between lipid membranes and several annexins by cryo-electron microscopy, J. Mol. Biol. 272 (1997) 42–55.
[6] S.E. Moss, in: S.E. Moss (Ed.), The Annexins, Portland Press, London, 1992.
[7] P. Raynal, H.B. Pollard, Annexins: the problem of assessing the biological role for a gene family of multifunctional calcium- and phospholipid-binding proteins, Biochim. Biophys. Acta 1197 (1994) 63–93.
[8] W.S. Maillard, H.T. Haigler, D.D. Schlaepfer, Calcium-dependent binding of S100C to the N-terminal domain of annexin I, J. Biol. Chem. 271 (1996) 719–725.
[9] V. Gerke, K. Weber, Identity of p36K phosphorylated upon Rous sarcoma virus transformation with a protein purified from the brush border; calcium-dependent binding to non-erythroid spectrin and F-actin, EMBO J. 3 (1984) 227–233.
[10] H. Tokumitsu, A. Mizutani, H. Minami, R. Kobayashi, H. Hidaka, A calcyclin-associated protein is a newly identifies member of the Ca^{2+}/phospholipid-binding proteins, annexin family, J. Biol. Chem. 267 (1992) 8919–8924.
[11] T. Becker, K. Weber, N. Johnsson, Protein-protein recognition via short amphiphilic helices; a mutational analysis of the binding site of annexin II for p11, EMBO J. 9 (1990) 4207–4213.
[12] S. Réty, J. Sopkova, M. Renouard, D. Osterloh, V. Gerke, S. Tabaries, F. Russo-Marie, A. Lewit-Bentley, Crystal structure of a complex of p11 with the annexin II N-terminal peptide, Nat. Struct. Biol. 6 (1999) 89–95.
[13] N. Johnsson, G. Marriott, K. Weber, p36, the major cytoplasmic substrate of src tyrosine protein kinase, binds to its

p11 regulatory subunit via a short amino-terminal amphipathic helix, EMBO J. 7 (1988) 2435–3442.
[14] E. Kube, T. Becker, K. Weber, V. Gerke, Protein–protein interaction studied by site-directed mutagenesis, J. Biol. Chem. 267 (1992) 14175–14182.
[15] N. Johnsson, K. Weber, Alkylation of cysteine 82 of p11 abolishes the complex formation with the tyrosine-protein kinase substrate p36 (annexin 2, calpactin 2, lipocortin 2), J. Biol. Chem. 265 (1990) 14464–14468.
[16] A. Burger, R. Berendes, S. Liemann, J. Benz, A. Hofmann, P. Göttig, R. Huber, V. Gerke, C. Thiel, J. Römisch, K. Weber, The crystal structure and ion channel activity of human annexin II, a peripheral membrane protein, J. Biol. Chem. 257 (1996) 839–847.
[17] D.M. Waisman, Annexin II tetramer: structure and function, Mol. Cell. Biochem. 149/150 (1995) 301–322.
[18] B.R. Brooks, R.E. Bruccoleri, B.D. Olafson, D.J. States, S. Swaminathan, M. Karplus, CHARMM: A program for macromolecular energy, minimization and dynamics calculations, J. Comput. Chem. 4 (1983) 187–217.
[19] J. Cherfils, S. Duquerroy, J. Janin, Protein–protein recognition analyzed by docking simulations, Proteins 11 (1991) 271–280.
[20] S.J. Wodak, J. Janin, Computer analysis of protein–protein interactions, J. Mol. Biol. 124 (1987) 323–342.
[21] CCP4. Collaborative Computational Project Number 4. The CCP4 suite: programs for protein crystallography. Acta Cryst. D50 (1994) 760–763.
[22] A.D. Mackerell, D. Bashford, M. Bellott, R.L. Dunbrack Jr., J. Evenseck, M.J. Field, S. Fisher, J. Gao, H. Guo, S. Ha, D. Joseph, L. Kuchnir, K. Kuzcera, F.T.K. Lau, C. Mattos, S. Michnick, T. Ngo, D.T. Nguyen, B. Prodhom, I.W.E. Reiher, B. Roux, M. Schlenkrich, J.C. Smith, R. Stote, J. Straub, M. Watanabe, J. Wiorkiewicz-Kuczera, D. Yin, M. Karplus, All-atom empirical potential for molecular modeling and dynamics studies of proteins, J. Phys. Chem. B 102 (1998) 3586–3616.
[23] S. Réty, D. Osterloh, J.P. Arie, S. Tabaries, J. Seeman, F. Russo-Marie, V. Gerke, A. Lewit-Bentley, Structural basis of the Ca^{2+}-dependent association between S100C (S100A11) and its target, the N-terminal part of annexin I, Struct. Fold. Des. 8 (2000) 175–184.
[24] P.J. Kraulis, MOLSCRIPT: a program to produce both detailed and schematic plots of protein structures, J. Appl. Cryst. 24 (1991) 946–950.